中國機械工程學刊第四十四卷第四期第 301~310 頁(民國一百一十二年)
Journal of the Chinese Society of Mechanical Engineers, Vol.44, No.4, pp301~310 (2023)

Optimization Design of a Three-Piece Dental Implant System by Uniform Design and Gray Relation Analysis

Danang Yudistiro* and Yung-Chang Cheng**

Keywords： Three-piece dental implant, Fatigue safety factor, Uniform design, Gray relation analysis.

ABSTRACT

This study improves the strength of dental implant system under the fatigue and torsion testing simulation. The fatigue safety factor and the von Mises stress for a three-piece implant model are evaluated via ANSYS software. Control factors are continuous in the design space so a uniform design (UD) is used to construct a group of simulation experiments. Kriging interpolation (KGI) is utilized to create the Kriging surrogate model (KGSM). In the multi-objective optimization strategy, the entropy weighting method (EWM), gray relation analysis (GRA) and genetic algorithm (GA) are integrated to obtain the optimal solution and values. Finally, after executing the UD and multi-objective optimization techniques, the fatigue safety factor of the optimal design has been increased to1.791, the von Mises stress is reduced to 364.65 MPa. Further, it shows a 29.59 % and 7.74 % improvement for the fatigue safety factor and von Mises stress compared with the original design.

INTRODUCTION

Dental implants have long been used as a treatment for tooth decay. One of the factors that influence the success of dental implant placement is the reliability of the bond between the implant and the surrounding bone (Sharma et al., 2020). Stable implant and bone bonds will greatly affect osseointegration. Osteointegration is one issue that is faced. Topkaya et al., (2015) proposed that osseointegration be given more attention when developing dental implants. Because dental implants are not as strong as natural teeth, good dental implant design is one of the keys. Therefore, good implant design selection is important and can affect primary stability and osseointegration (Gehrke et al., 2019). Good implant design aims to make the patient satisfied in terms of geometric design and structural robustness.

Dental implant design has been the subject of numerous studies. Numerous research has examined the stability of osseointegration, static stress, and displacement (Cheng et al., 2015; Manchikalapudi & Basapogu, 2022; Jiang et al., 2014; Milone et al., 2022; Paracchini et al., 2020) To investigate the stress distribution in the cortical and cancellous bone around two dental implant models, Paracchini et al. (2020) used finite element analysis. Milone et al. (2022) analyzed the comparison of stress distribution between zirconia and titanium dental implants. The method used is ANSYS software. Manchikalapudi and Basapogu (2022) used the ANSYS program to analyze the stress distribution on two types of implants with different crown materials. Additionally, micromotion (displacement) in cortical bone and cancellous bone under dynamic chewing loads may be calculated using ANSYS/LS-DYNA (Cheng et al., 2015; Jiang et al., 2014).

Calculating fatigue life is the critical factor in calculating dental implant strength. There have been numerous studies on the effects of fatigue on life and behavior (Ayllón et al., 2014; Geramizadeh et al., 2018; Liu et al., 2016; Prados-Privado et al., 2019; Darwich et al., 2022; Bayata and Yildiz, 2020). Appling ANSYS software, Ayllón et al. (2014) investigated the fatigue behaviour and the stress intensity factor of the titanium dental implants. Using ANSYS software, Geramizadeh et al. (2018) evaluated the fatigue life of a dental implant model involved V-shaped threads. The

Paper Received February, 2023. Revised April, 2023. Accepted April, 2023. Author for Correspondence: Yung-Chang Cheng.

* *Graduate student, Ph. D. Program in Engineering Science and Technology, College of Engineering, National Kaohsiung University of Science and Technology, Taiwan 824, ROC.*

** *Corresponding author: Professor, Department of Mechatronics Engineering, National Kaohsiung University of Science and Technology, Kaohsiung, Taiwan 824, ROC.*

standard for assessing the fatigue limit and failure probability is ISO 14801. ANSYS/Workbench software and a titanium dental implant model were used in the study by Prados-Privado et al., (2019) and Liu et al., (2016). Darwich et al. (2022) completed research on fatigue stress with a custom-made all-on-4 implants system object by ANSYS software. Based on Finite Element Analysis (FEA), the failure analysis of Ti-6Al-4V implant systems was performed under real biting forces according to ISO 14801 by Bayata and Yildiz (2020).

Reducing von Mises stress and deformation is one of the design optimization attempts. The von Mises stress and the deformation have been the subject of numerous investigations. The von Mises stress and deformation are essential in determining whether a dental implant is ideal, but they are not the only ones. Torsion plays a significant role in dental implant surgery, and torsion testing simulation is crucial for designing dental implants.

The study calculates the fatigue safety factor and von Mises stress of a dental implant model using ISO 14801 fatigue and ISO 13498 torsion testing standards. To improve the design of the three-piece dental implant system, the uniform design of experiment is used to conduct a series of simulated experiments in the design space. Using SolidWorks, a 3D model of the three-part dental implant system (abutment, abutment screw, and implant) is created. The minimum fatigue safety factor and the maximum von Mises stress for each implant model are determined using ANSYS/Workbench software for fatigue and torsion testing simulations. The uniform table is then used to find the single optimal solution by KGI and GA techniques. The multi-objective optimization results are obtained by integrating EWM, GRA, and GA. The predicted and real analyzed results are compared, and the optimal design model and analysis results are finally obtained.

FINITE ELEMENT ANALYSIS

Three-Piece Dental Implant Model

Figure 1 depicts the reconstruction of the three-piece dental implant base's geometric design using SolidWorks software. This three-piece dental implant system is referred to as the modified C-Tech dental implant system (Lerner, 2018) and comprises the dental implant, abutment, and abutment screw. The dental implant has a trapezium shape and a thread type. The critical parameters used in the design are thread length (TL), main diameter (MD), basic screw diameter (BSD), main thread pitch (MTP), secondary thread pitch (STP), and main thread depth (MTD), as shown in Table 1 and depicted in Figure 2.

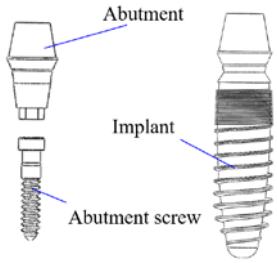

Figure 1. 3D model of the three-piece dental implant

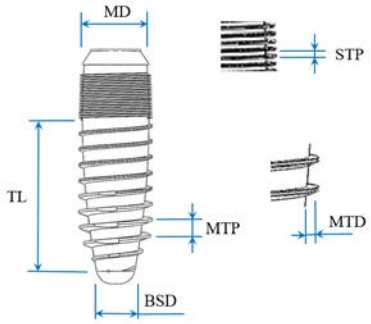

Figure 2. Geometric dimensions of the dental implant model

Table 1. Geometric properties of the three-piece implant system

Basic screw diameter **BSD** **(mm)**	Main diameter **MD** **(mm)**	Secondary thread pitch **STP** **(mm)**	Thread length **TL** **(mm)**	Main thread pitch **MTP** **(mm)**	Main thread depth **MTD** **(mm)**
2.1	4.3	0.2	9.7	1.0	0.3

Fatigue Finite Element Modeling

The Organization for International Standardization developed the standard for fatigue testing in 2003. In this paper, the fatigue finite elements analysis (FEA) is conducted using the ISO 14801 standard. The axial load acting on the cap is 300 N. Figure 3 shows the setup for the FEA for dental implants according to the ISO 14801 standard. The fatigue tests in this study utilize fixed clamping devices and employ rigid and fixed clamping mechanisms.

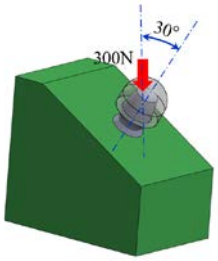

Figure 3. Fatigue testing of a dental implant for the ISO 14801 standard

The safety component functions as the performance index for the fatigue test in this study.

The safety factor represents the ratio of the structure's load-bearing capacity to the predicted load, which can come from static, dynamic, and impact forces, among others. The fatigue test safety factor is used to anticipate mechanical failure of dental implants and ensure the structural design does not fail. In this study, a dental implant is considered structurally safe if it has a safety factor greater than 1.

For the fatigue testing simulation analysis, Table 2 shows the mechanical properties of four sections, including the implant, the abutment, the holder, and the cap. Utilizing Ti6Al4V, the implant, abutment, and abutment screw are built. Figure 4 shows the Ti6Al4V SN-curve for the fatigue finite element calculations. (Janeček et al., 2015).

Table 2. Mechanical Properties of the dental implant testing system

Component	Density (kg/mm^3)	Young's modulus (MPa)	Poisson's ratio
Implant, Abutment, Abutment screw	4.5×10^{-6}	1.1×10^{5}	0.35
Cap	8×10^{-6}	1.93×10^{5}	0.25
Holder	4.5×10^{-6}	3.5×10^{3}	0.3
Specimen holder	7.85×10^{-6}	2×10^{5}	0.3

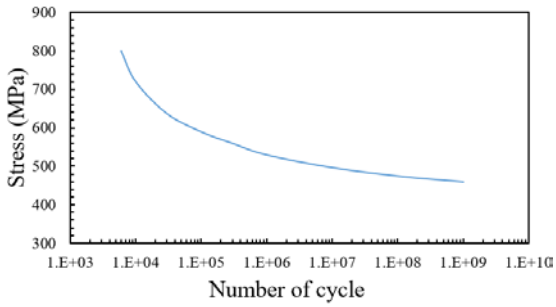

Figure 4. The SN-curve for Ti6Al4V

The ISO 14801 testing standard specifies a boundary condition for the fatigue finite element analysis, as illustrated in Figure 5(a). The cap undergoes an external loading that is applied vertically. The minimum fatigue safety factor is calculated using ANSYS/Workbench software. The accuracy is enhanced through a convergence analysis for element meshing, where the size of the elements is determined based on changes in the magnitude of the fatigue safety factor for various distinct elements. If the difference in analysis results between two elements is less than 5%, it indicates that the analysis result has converged for all chosen elements.

Figure 5(b) displays the results for various elemental sizes. A size of 0.25 mm is deemed optimal because the difference in simulation results between 0.25 and 0.2 mm is less than 5%. Figure 5(c) displays the fatigue safety factor for this optimal elemental size, with a minimum fatigue safety factor of 1.382. This simulated endurance test demonstrates that the dental implants are safe for use.

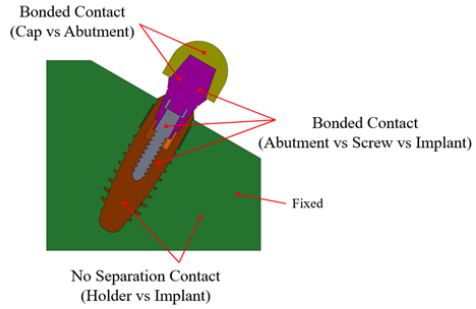

(a)

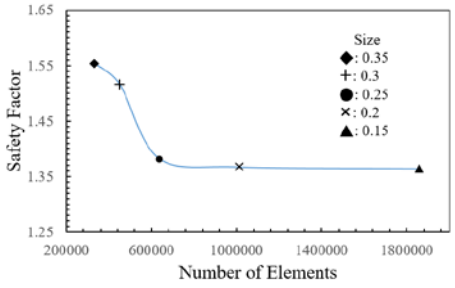

(b)

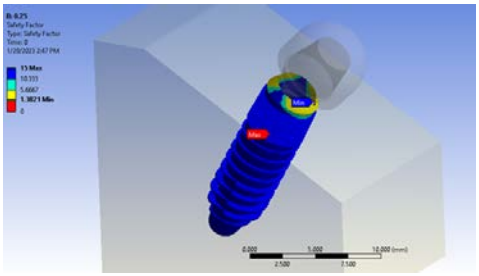

(c)

Figure 5. (a) Setting for boundary conditions in FEA system, (b) the convergence analysis of the fatigue safety factor for various element sizes and (c) the fatigue safety factor distributions for the fatigue test simulation

Torsion Finite Element Modeling

Torsion testing is a crucial component of standard testing for dental implants. The process typically begins with the attachment of a dental implant body to the jawbone, followed by the attachment of other parts to create a dental prosthetic. The components must be securely attached to the dental implant body and able to withstand masticatory loads, including torsional loads.

In order to evaluate the torsional yield

strength and maximum torque on a dental implant body or connecting endosseous dental implants, ISO 13498 (2011) was established in 2011. The implant body and connecting components are secured in a testing apparatus in accordance with this standard to determine the torsional yield strength and maximum
torque. The maximum bond holder distance used to connect the implant body/connection to the specimen holders is 5mm. A static structural moment component of 1.533 N-m, which is a fixed part, is applied in one section. Figure 6 illustrates a typical torque test performed using a torsion testing apparatus.

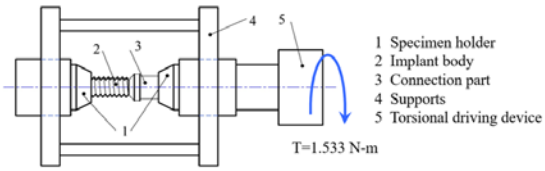

Figure 6. Torsion testing for the ISO 13498 standard

The torsion test simulation for ISO 13498 uses boundary conditions, as depicted in Figure 7(a). A torsional drive device is utilized to apply horizontal torsion to the specimen holder. Figure 7(b) showcases the results for various elemental sizes, and it is determined that an elemental size of 0.25 mm is optimal, as the difference between the simulation results for 0.25 and 0.2 mm is less than 5%. The von Mises stress for this ideal elemental size is displayed in Figure 7(c), with the maximum von Mises stress for the dental implant system being 395.24 MPa.

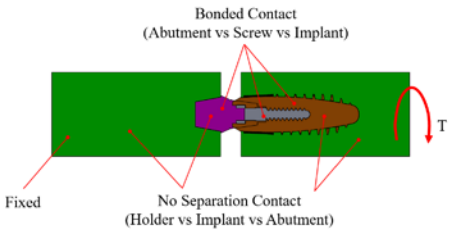

(a)

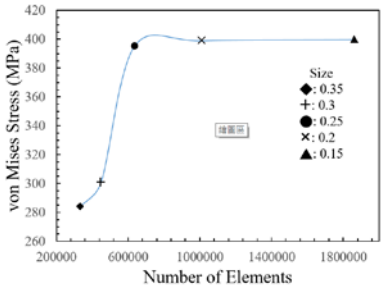

(b)

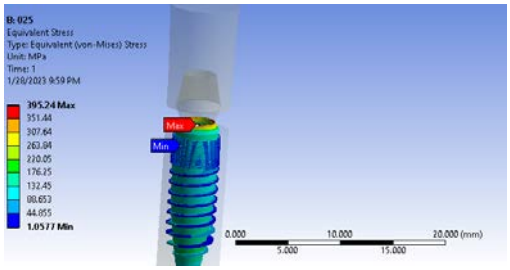

(c)

Figure 7. (a) Setting for boundary conditions in FEA system, (b) the convergence analysis of the von Mises stress for various element sizes and (c) the von Mises stress distributions for the torsion test simulation.

MULTI-OBJECTIVE OPTIMIZATION DESIGN OF AN IMPLANT

Uniform Design of Experiment

The primary stability and osseointegration of implants are essential factors in this study's discussion of the thread parameter. (Park et al., 2009). This study uses several key characteristics. Table 3 shows some of the key design features of dental implants. Six control factors are used for the dental implant system: ITD, ITP, ATD, ATP, ABS and ATL.

The design space is considered continuous because, as shown in Table 3, the control factors are continuous. As a result, the uniform design of experiments approach is employed to create a set of sample points that are evenly distributed in the continuous design space. (Fang and Wang, 1994) The uniform design method is a commonly used technique in several engineering fields. (Song et al, 2016; Zhang et al, 2018; Lee et al, 2015) This approach requires fewer simulations to be run, thus saving time while improving quality and efficiency. The finite element analysis simulation is utilized to determine the fatigue safety factor and von Mises stress values, which are then uniformly distributed. The levels of other components in the simulation process are determined based on the uniformity of these values. A uniform design provides more information compared to simulations with fewer simulated samples.

Table 3. Design ranges for the control factors

Control Factor	Lower bound	Basic Value	Upper Bound
ITD (mm)	0.3	0.45	0.6
ITP (mm)	0.5	0.75	1
ATD (mm)	0.3	0.4	0.5
ATP (mm)	0.3	0.75	1.2
ABS (mm)	1	1.25	1.5
ATL (mm)	4	5.5	7

The Kriging model's accuracy improves as

the number of experiments increases, but this also requires more computational time. Hence, the number of experiments is limited. The minimum number of experiments required to start the Kriging model is determined by the minimum number of input points needed. The Kriging model needs to be initialized with at least 2n+1 design points, where n is the number of inputs. In this study, n inputs are used, so the minimum number of experiments, m, is calculated as 2n+1, which is m=2n+1. To optimize the simulation process while considering the restrictions of machine instrumentation, a uniform design of experiment (Fang and Wang, 1994) was used and each factor was assigned 18 levels. This resulted in 18 simulation tests being created using the uniform table $U_{18}^{*}\left(18^{11}\right)$.

The uniform design table $U_{18}^{*}\left(18^{11}\right)$ (Fang and Wang, 1994) is employed to conduct sixteen experiments, as illustrated in Table 4. Six control factors were considered in this implant design, including implant thread depth, pitch, abutment thread depth, pitch, abutment body size, and abutment thread length, and these factors were utilized in the uniform design table. The results of the sixteen experiments are displayed in Table 4. The 3D solid dental implant model for each experiment was created utilizing the SolidWorks geometric tool, and the simulation tests were carried out using ANSYS/Workbench. The results for the fatigue safety factor and the von Mises stress for the ISO 14801 and ISO 13498 tests, respectively, are presented in Table 4.

In terms of simulation results, the original model has a fatigue safety factor of 1.38 in the fatigue test simulation and a von Mises stress of 395.24 MPa in the torsion test simulation. The 16th experiment has improved the fatigue safety factor to 1.741, while the 4th experiment has decreased the von Mises stress to 345.61 MPa. However, these two results are not from the same experiment, thus requiring the use of a multi-objective optimization method to achieve the best design outcome.

Table 4. (a) The experimental uniform design and (b) simulation results

(a)

Exp. No.	ITD (mm)	ITP (mm)	ATD (mm)	ATP (mm)	ABS (mm)	ATL (mm)
1	1.900	4.120	0.204	9.35	1.082	0.365
2	1.935	4.290	0.233	11.23	1.400	0.318
3	1.971	4.470	0.262	8.64	1.047	0.271
4	2.006	4.650	0.180	10.52	1.365	0.224
5	2.041	4.820	0.209	7.94	1.012	0.400
6	2.076	5.000	0.239	9.82	1.329	0.353
7	2.112	4.060	0.268	11.70	0.976	0.306
8	2.147	4.240	0.186	9.11	1.294	0.259
9	2.182	4.410	0.215	10.99	0.941	0.212
10	2.218	4.590	0.245	8.41	1.259	0.388
11	2.253	4.760	0.274	10.29	0.906	0.341
12	2.288	4.940	0.192	7.70	1.224	0.294
13	2.324	4.000	0.221	9.58	0.871	0.247
14	2.359	4.180	0.251	11.46	1.188	0.200
15	2.394	4.350	0.280	8.88	0.835	0.376
16	2.429	4.530	0.198	10.76	1.153	0.329
17	2.465	4.710	0.227	8.17	0.800	0.282
18	2.500	4.880	0.256	10.05	1.118	0.235

(b)

Exp. No.	Safety factor Y1	von Mises stress Y2 (MPa)
1	1.556	359.04
2	1.426	375.64
3	1.735	402.47
4	1.479	345.61
5	1.610	396.26
6	1.714	364.18
7	1.320	386.87
8	1.393	351.87
9	1.461	419.91
10	1.470	399.94
11	1.426	386.76
12	1.627	375.54
13	1.530	380.31
14	1.476	379.66
15	1.548	391.80
16	1.741	369.65
17	1.559	402.31
18	1.500	370.43

Surrogate Model Creation

When the direct evaluation of a result of interest is not feasible, a surrogate model is used to model the outcome. In this technique, output data is collected from complex system simulations, and surrogate models are developed to statistically link input data to output data. This study employs Kriging Interpolation (KGI), a stochastic interpolation method, to transform discrete experimental data into a continuous model. KGI has been widely used in engineering problems and is capable of handling a certain amount of noise and various types of experimental results. (Gu et al., 2007; Lee et al., 2015; McLean et al., 2006; Simpson et al., 2001)

Based on the Gaussian correlation function and zero-order regression, the Kriging surrogate model (KGSM) of the unknown response function can be expressed as the following equation: The

following equation is the Kriging surrogate model (KGSM) $\hat{y}(\mathbf{x})$ of the unknown response function $y(\mathbf{x})$ based on the Gaussian correlation function and zero-order regression. (Lophaven et al., 2012) :

$$\hat{y}(\mathbf{x}) = \beta + \mathbf{r}^T(\mathbf{x})\mathbf{R}^{-1}(\mathbf{Y} - \mathbf{F}\beta) \quad (1)$$

In equation (1), $\mathbf{x} = \{x_1, x_2, \cdots, x_p\}$ signifies a vector with unidentified input variables. The number of unknown variables is p. $\mathbf{r}(\mathbf{x})$ expresses an n-dimensional vector and is a function of the unidentified input variables. For an unknown function, $\mathbf{Y} = \{y_1, y_2, \ldots, y_n\}^T$ denotes a known response vector. $\mathbf{F}$ is an n-dimensional column vector with all ones. $\mathbf{R} = \left[R_{ij}\right]_{n\times n}$ indicates a known square matrix and is evaluated by

$$R_{ij} = \prod_{m=1}^{p} \exp\left[-\theta_m \left(x_{im} - x_{jm}\right)^2\right], \quad (2)$$

$i = 1, 2, \cdots, n, \;\; j = 1, 2, \cdots, n$

Moreover, β specifies a known constant and is determined by

$$\beta = \left(\mathbf{F}^T\mathbf{R}\mathbf{F}\right)^{-1}\mathbf{F}^T\mathbf{R}\mathbf{Y} \quad (3)$$

In this study, the primary objective is to evaluate the fatigue safety factor and von Mises stress of the dental implant system. The input and output data obtained from the Uniform Design (UD) technique as presented in Table 4 are used to calculate the Kriging Surrogate Model (KGSM) of the target function. The calculation procedure is outlined in detail below:

$$\hat{y}_{\mathrm{m}}(\mathbf{x}) = \beta + \mathbf{r}^T(\mathbf{x})\mathbf{R}^{-1}(\mathbf{Y} - \mathbf{F}\beta) \quad (4)$$

Grey Relation Analysis

In the field of Grey system theory, the original GRA algorithm was developed by Deng (1982). GRA is employed in complex systems with multiple variables and components to tackle difficult problems. This analytical approach incorporates geometric computing and the criteria of ordinariness, regularity, and totality. GRA is utilized in various industries to establish the connections between a system's control variables and its analysis outcomes. (Hsiao et al, 2017; Kuo et al, 2008; Yamaguchi et al, 2005)

The input data is first normalized, and the grey relational coefficients are calculated. The grey relational grades (GRG) are then determined using the weight assigned to each objective function. The optimal weight for each objective function is determined using the EWA in this paper. The procedure for the Grey Relational Analysis (GRA) is illustrated in Figure 8, and further details can be found in the work of Huang and Lin (2009). The grey relational coefficients $\gamma_{0i}(j)$ and GRG Γ_{0i} are determined as:

$$\gamma_{0i}(j) = \frac{\Delta\min + \Delta\max}{\Delta_{0i}(j) + \Delta\max} \quad (5)$$

$$\Gamma_{0i} = \sum_{j=1}^{k} W_j \gamma_{0i}(j) \quad (6)$$

Where $\Delta_{0i}(j) = \left|x_0(j) - x_i(j)\right|$ is the difference in the absolute values of $x_0(j)$ and $x_i(j)$, $\Delta\max = \max_{\forall j} \Delta_{0i}(j)$ expresses the maximum value of $\Delta_{0i}(j)$, $\Delta\min = \min_{\forall j} \Delta_{0i}(j)$ is the minimum value of $\Delta_{0i}(j)$ and W_j is the weight of attribute *j*.

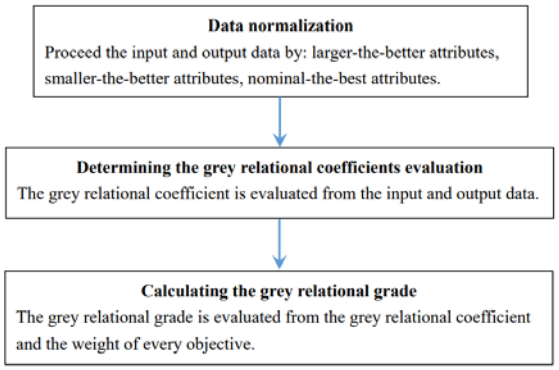

Figure 8. The evaluation process for GRA

Entropy Weight Analysis

This study uses an innovative methodology to achieve the multiple objective optimization design for an EABF, encompassing UD table, KGI, GA, EWA and GRA. Figure 10 shows the optimization design strategy to create the best design. The justification and the numerical results are detailed below.

Step 1. Using EWA and the UD results, calculate the appropriate weights.

The appropriate weight for each objective function from EWA, (0.54, 0.46), is determined using the FEA results given in Table 4.

Step 2. For a single objective optimization result, produce a KGS model using KGI and GA.

Using the UD results in Table 4 and KGI method, the KGS models have been generated to obtain each objective function. Applying the GA technique, the optimal value for each single objective function has been established as shown in Table 5.

Table 5. Optimal value for the single objective optimization design

Objective function	Y1	Y2 (MPa)
Optimal value	1.757	339.22

Figure 10. Multiple objective optimal design process

Step 3. Using GRA, the GRG is evaluated by the ideal weights from the step 1 and the normalized values of each objective function.

Applying the best value from Table 5, the UD outcomes in Table 4 for each objective function are normalized. Substituting the optimal weights that ae calculated using the EWA to the GRA method, the GRG is shown in Table 6.

Table 6. Results for the GRG

Experiment No.	Gray relation grade
1	0.640
2	0.494
3	0.738
4	0.701
5	0.558
6	0.803
7	0.426
8	0.605
9	0.420
10	0.454
11	0.462
12	0.629
13	0.533
14	0.504
15	0.516
16	0.840
17	0.503
18	0.549

Step 4. Using KGI and GA, calculate the optimal GRG and the optimal solution.

The KGI method is used to construct a GRG surrogate model. The functional linkages between the control variables and the objective function are built by KGI technique. The KGS model of the GRG value also describes the functional relationship. The optimal GRG and solution are determined using GA and the results are shown in Table 7. The optimal design for an EABF system is the geometrical dimensions of the ideal frame. The best GRG, which is greater than every other GRG in Table 6, is 0.842.

Table 7. Optimal solution and the GRG

Optimal solution for implant					
ITD (mm)	ITP (mm)	ATD (mm)	ATP (mm)	ABS (mm)	ATL (mm)
2.423	4.539	0.197	10.753	1.160	0.331

Step 5. Applying the KGS model for Y1 and Y2, the predicted value for each objective function is assessed.

The final optimization solution is shown in Table 7. In Table 8, the predicted optimal values for each objective function are clearly derived via the KGS model of Y1 and Y2. It contains the errors for the estimated optimal values and real analysis values for Y1 and Y2.

Step 6. The validation for the predicted and real simulated value by the software packages SolidWorks and ANSYS/Workbench.

Applying the SolidWorks and ANSYS/Workbench software, the real fatigue safety factor for the fatigue test simulation and the real von Mises stress for the torsion test simulation of the optimal implant model is determined. The errors between the predicted and the actual values for Y1 and Y2 are shown in Table 8. The respective predicted errors for Y1 and Y2 are 2.11 % and 0.65 %. The optimization process is complete because all of the predicted errors are less than 3%. The fatigue safety factor and von Mises stress for the optimal design of an implant model are illustrated as shown in Figure 11.

Table 8. Optimal predicted value and predicted error

Objective function	Predicted value	Real value	Predicted error (%)
Y1	1.754	1.791	2.11
Y2 (MPa)	367.03	364.65	0.65

Table 9 shows the fatigue safety factor and von Mises stress values and increments for various phases. The fatigue safety factor is 1.741 after the

UD of experiment. Moreover, the von Mises stress is improved to 369.65 MPa after the UD of experiment. The respective improvements in Y1 and Y2 are 25.97 % and 6.47 %. The fatigue safety factor increases to 1.791 after the multiple objective optimization and the von Mises stress decreases to 364.65 MPa. The respective improvements in Y1 and Y2 are 29.59 % and 7.74 %. All of the fatigue safety factor and von Mises stress for the ISO 14801 and ISO 13498 test simulations show an improvement.

Table 9. FEA values and improvement rate for various phases

Phase	Objective function	Analysis value	Error (%)
Original design	Y1	1.382	—
	Y2 (MPa)	395.24	—
After UD technique	Y1	1.741	25.97
	Y2 (MPa)	369.65	6.47
After multi-objective optimization	Y1	1.791	29.59
	Y2 (MPa)	364.65	7.74

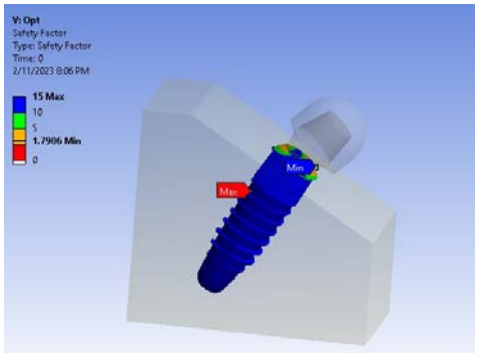

(a)

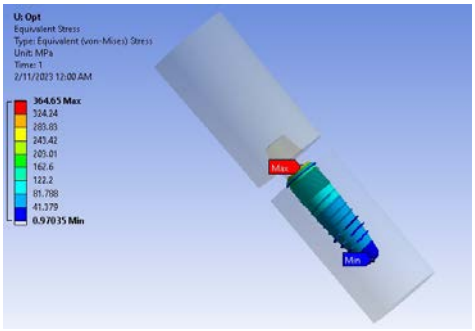

(b)

Figure 11. The distribution of (a) the fatigue safety factor and (b) the von Mises stress for the improved design for fatigue and torsion testing simulations.

CONCLUSION

This study investigates the strength of a three-piece dental implant system using ANSYS/Workbench software. The fatigue safety factor and the von Mises stress are calculated based on the ISO 14801 and 13498 testing standards, respectively. The optimal elemental size for each implant model is determined through a convergence study by analyzing the meshing quality of the finite element analysis using different elemental sizes. Using UD and KGI techniques, the KGSMs of the fatigue safety factor and von Mises stress are obtained. Integrating EWM, GRA and GA process, the optimization design of a three-piece dental implant system is completely found. The optimization led to an increase of 29.59% in the fatigue safety factor and 7.74% in the von Mises stress, resulting in a superior dental implant system compared to the original design. As a result, the multi-objective optimization design procedure that is suggested results in a design for the three-piece dental implant system.

ACKNOWLEDGMENTS

The authors extend their sincere gratitude to the Ministry of Science and Technology (MOST) for their financial support through grant numbers 111-2221-E-992-057.

REFERENCE

Ayllón J. M., Navarro C., Vázquez J. and Domínguez J.. “Fatigue life estimation in dental implants,” Engineering Fracture Mechanics, Vol.123, pp.34–43 (2014).

Ayşegül T. I. and Esra A. A., “The decision-making approach based on the combination of entropy and Rov methods for the apple selection problem,” European Journal of Interdisciplinary Studies, Vol. 3, No. 3, pp. 80-86 (2017).

Bayata F. and Yildiz C., “The effects of design parameters on mechanical failure of Ti-6Al-4V implants using finite element analysis,” Engineering Failure Analysis, Vol.110, pp.104445-1~104445-37 (2020).

Cheng Y. C., Lin D. H., Jiang C. P. and Lee S. Y., “Design improvement and dynamic finite element analysis of novel ITI dental implant under dynamic chewing loads,” Bio-Medical Materials and Engineering, Vol. 26, No. s1, pp.S555–S561 (2015).

Clausius R., “Ueber verschiedene für die Anwendung bequeme Formen der Hauptgleichungen der mechanischen Wärmetheorie,” Annalen der Physik und Chemie, Vol. 201, No. 7, pp.353–400 (1865).

Darwich A., Alammar A., Heshmeh O., Szabolcs S. and Nazha H., “Fatigue loading effect in custom-made all-on-4 implants system: A 3D finite elements analysis,” Innovation and Research in BioMedical Engineering,

Vol. 43, No. 5, pp.372–379 (2022).
Deng J. L., "Control problems of grey systems," Systems & Control Letters, Vol. 1, No. 5, pp. 288–294 (1982).
Fang K. and Wang Y., Number-theoretic methods in statistics (1st ed). London ; New York: Chapman & Hall. (1994).
Gehrke S. A., Eliers Treichel T. L., Pérez-Díaz L., Calvo-Guirado J. L., Aramburú Júnior J., Mazón P. and de Aza P. N., "Impact of different titanium implant thread designs on bone healing: A biomechanical and histometric study with an animal model," Journal of Clinical Medicine, Vol. 8, No. 6, pp. 777-1~777-12 (2019).
Geramizadeh M., Katoozian H., Amid R. and Kadkhodazadeh M., "Comparison of finite element results with photoelastic stress analysis around dental implants with different threads," Dental and Medical Problems, Vol. 55, No. 1, pp. 17–22 (2018).
Gu Y. T., Wang Q. X. and Lam K. Y., "A meshless local Kriging method for large deformation analyses," Computer Methods in Applied Mechanics and Engineering, Vol. 196, No. 9–12, pp. 1673–1684 (2007).
Hsiao S. W., Lin H. H. and Ko Y. C., "Application of grey relational analysis to decision-making during product development," EURASIA Journal of Mathematics, Science and Technology Education, Vol. 13, No. 6, pp. 2581-2600 (2017).
Huang Y. L. and Lin C. T., "Constructing grey relation analysis model evaluation of tourism competitiveness," Journal of Information and Optimization Sciences, Vol. 30, No. 6, pp. 1129–1138 (2009).
Işık A. T. and Adalı E. A., "The decision-making approach based on the combination of entropy and Rov methods for the apple selection problem," European Journal of Interdisciplinary Studies, Vol. 3, No. 3, pp.80-86 (2017).
ISO 14801. Fatigue Test for Endosseous Dental Implants. International Organization for Standardization; 2013.
ISO 13498. Dentistry — Torsion test of implant body/connecting part joints of endosseous dental implant systems; 2011.
Janeček M., Nový F., Harcuba P., Stráský J., Trško L., Mhaede M. and Wagner L., "The very high cycle fatigue behaviour of Ti-6Al-4V alloy," Acta Physica Polonica A, Vol. 128, No. 4, pp. 497–503 (2015).
Jiang C. P., Lee C. K., Tsai W. L. and Cheng Y. C., "Uniform design and dynamic finite element analysis for micromotion improvement of semados dental implant system under dynamic chewing loads," Journal of Mechanics in Medicine and Biology, Vol. 14, No. 6, pp.1440007-1~1440007-9 (2014).
Kuo Y., Yang T. and Huang G. W., "The use of grey relational analysis in solving multiple attribute decision-making problems," Computers & Industrial Engineering, Vol. 55, No. 1, pp. 80–93 (2008).
Lee C. K., Cheng Y. C. and Jiang C. P., "Explicit dynamic finite element analysis and uniform design with kriging interpolation and optimization to improve an on-road bicycle frame undergoing drop-mass impact test," Journal of the Chinese Society of Mechanical Engineers, Vol. 36, No. 4, pp. 353–361 (2015).
Lerner H., Lorenz J., Sader R. A. and Ghanaati S., "Peri-implant health and peri-implant bone stability after immediate implant placement," Modern Research in Dentistry, Vol. 3, No. 1, pp. 213-223 (2018).
Liu L., Zhang X., Zhou Y. F., Chen X. S. and Wang Y. L., "Influence on fatigue and biomechanics of cone fit of dental implant around the surrounding bone tissue," Materials Science Forum, Vol. 872, pp. 281–286 (2016).
Lophaven S., Nielsen H. and Søndergaard J., "DACE: A MATLAB Kriging Toolbox," Informatics and Mathematical Modelling Technical Report (2012).
Manchikalapudi G. and Basapogu S., "Finite element analysis of effect of cusp inclination and occlusal contacts in PFM and PEEK implant-supported crowns on resultant stresses," Medical Journal Armed Forces India, Vol. 78, No. 1, pp. 80–87 (2022).
McLean P., Léger P. and Tinawi R., "Post-processing of finite element stress fields using dual kriging based methods for structural analysis of concrete dams," Finite Elements in Analysis and Design, Vol. 42, No. 6, pp. 532–546 (2006).
Milone D., Fiorillo L., Alberti F., Cervino G., Filard V.i, Pistone A., Cicciù M. and Risitano G., "Stress distribution and failure analysis comparison between Zirconia and Titanium dental implants," Procedia Structural Integrity, Vol. 41, pp. 680–691 (2022).
Paracchini L., Barbieri C., Redaelli M., Croce D. D., Vincenzi C. and Guarnieri R., "Finite element analysis of a new dental implant design optimized for the desirable stress distribution in the surrounding bone region," Prosthesis, Vol. 2, No. 3, pp.

225–236 (2020).
Park J. H., Lim Y. J., Kim M. J. and Kwon H. B., “The effect of various thread designs on the initial stability of taper implants,” The Journal of Advanced Prosthodontics, Vol. 1, No. 1, pp. 19-25 (2009).
Prados-Privado M., Ivorra C., Martínez-Martínez C., Gehrke S. A., Calvo-Guirado J. L., and Prados-Frutos J. C., “A finite element analysis of the fatigue behavior and risk of failure of immediate provisional implants,” Metals, Vol. 9, No. 5, pp. 535 (2019).
Sharma C., Kalra T., Kumar M., Bansal A. and Chawla A. K., “To evaluate the influence of different implant thread designs on stress distribution of osseointegrated implant: A three-dimensional finite-element analysis study–An in vitro study,” Dental Journal of Advance Studies, Vol. 8, No. 1, pp. 9–16 (2020).
Simpson T. W., Mauery T. M., Korte J. J. and Mistree F., “Kriging models for global approximation in simulation-based multidisciplinary design optimization,” AIAA Journal, Vol. 39, No. 12, pp. 2233–2241 (2001).
Song G., Xu G., Quan Y., Yuan Q. and Davies P. A., “Uniform design for the optimization of Al_2O_3 nanofilms produced by electrophoretic deposition,” Surface and Coatings Technology, Vol. 286, pp. 268–278 (2016).
Tan J., Zhao H., Yang R., Liu H., Li S. and Liu J., “An entropy-weighting method for efficient power-line feature evaluation and extraction from LiDAR point clouds,” Remote Sensing, Vol. 13, No. 17, pp. 3446-1~3446-24 (2021).
Topkaya T., Solmaz M. Y., Dündar S., and Eltas A., “Numerical analysis of the effect of implant geometry to stress distributions of dental implant system,” Cumhuriyet Dental Journal, Vol. 18, No. 1, pp.17-24 (2015).
Vatansever K. and Akgűl Y., “Performance evaluation of websites using entropy and grey relational analysis methods: The case of airline companies,” Decision Science Letters, Vol. 7, No. 2, pp.119–130 (2018).
Yamaguchi D., Li G. D. and Nagai M., “New grey relational analysis for finding the invariable structure and its applications,” Journal of Grey System, Vol. 8, No. 2, pp. 167-178 (2005).
Zhang H., Lin H. and Zheng Y., “Application of uniform design method in the optimization of hydrothermal synthesis for nano MoS_2 catalyst with high HDS activity,” Catalysts, Vol. 8, No. 12, pp. 654-1~654-15 (2018).
Zhe W., Xigang X. and Feng Y., “An abnormal phenomenon in entropy weight method in the dynamic evaluation of water quality index,” Ecological Indicators, Vol. 131, pp. 108-137 (2021).
Zhu Y., Tian D. and Yan F., “Effectiveness of entropy weight method in decision-making,” Mathematical Problems in Engineering, Vol. 2020, pp. 3564835-1~3564835-5 (2020).

利用均勻設計與灰關聯分析法於三件式牙根之最佳設計

余達南、鄭永長
國立高雄科技大學機電工程系

摘 要

本研究使用疲勞和扭轉測試模擬分析，提高了牙根系統的強度。利用ANSYS 軟體，進行三件式牙根模型的疲勞安全係數和 von Mises 應力評估與計算。因為全部的控制因子在設計空間中是連續的，所以，採用均勻實驗設計(UD)來構建一組模擬實驗。使用Kriging插值法(KGI)建利克利金代理模型(KGSM)。在多目標最佳化過程中，結合了熵權法(EWM)、灰關聯分析(GRA)和基因演算法(GA)來得到最佳解和最佳值。最後，在執行UD和多目標最佳化流程後，最佳設計的疲勞安全係數提高到1.791，von Mises應力降低到364.65 MPa。 此外，與原始設計相比，疲勞安全係數和 von Mises 應力分別提高了 29.59%和 7.74%。